The Binding of CD93 to Multimerin-2 Promotes Choroidal Neovascularization

Gian Marco Tosi,[1] Giovanni Neri,[1] Stefano Barbera,[2] Lucia Mundo,[3] Barbara Parolini,[4] Stefano Lazzi,[3] Roberta Lugano,[5] Evelina Poletto,[6] Lorenzo Leoncini,[3] Grazia Pertile,[7] Maurizio Mongiat,[6] Anna Dimberg,[5] Federico Galvagni,[2] and Maurizio Orlandini[2]

[1]Ophthalmology Unit of the Department of Medicine, Surgery and Neuroscience, University of Siena, Siena, Italy
[2]Department of Biotechnology, Chemistry and Pharmacy, University of Siena, Siena, Italy
[3]Department of Medical Biotechnology, Section of Pathology, University of Siena, Siena, Italy
[4]Vitroretinal Unit, Sant'Anna Hospital, Brescia, Italy
[5]Department of Immunology, Genetics and Pathology, Science for Life Laboratory, Rudbeck Laboratory, Uppsala University, Uppsala, Sweden
[6]Department of Research and Diagnosis, Division of Molecular Oncology, Centro di Riferimento Oncologico di Aviano, IRCCS, Aviano, Italy
[7]IRCCS Sacro Cuore Don Calabria Hospital, Negrar (VR), Italy

PURPOSE. The purpose of this study was to investigate the involvement of CD93 and Multimerin-2 in three choroidal neovascularization (CNV) models and to evaluate their contribution in the neovascular progression of age-related macular degeneration (AMD).

METHODS. Choroidal neovascular membranes collected during surgery from AMD patients were analyzed by microscopy methods. Laser-induced CNV mouse models and choroid sprouting assays (CSAs) were carried out using the CD93 knockout mouse model. An original ex vivo CSA of vascular angiogenesis, employing choroid tissues isolated from human donors, was developed.

RESULTS. In contrast to healthy choroid endothelium, hyperproliferative choroidal endothelial cells (ECs) of AMD patients expressed high levels of CD93, and Multimerin-2 was abundantly deposited along the choroidal neovasculature. CD93 knockout mice showed a significant reduced neovascularization after laser photocoagulation, and their choroidal ECs displayed a decreased ability to produce sprouts in ex vivo angiogenesis assays. Moreover, the presence of an antibody able to hamper the CD93/Multimerin-2 interaction reduced vascular sprouting in the human CSA.

CONCLUSIONS. Our results demonstrate that CD93 and its interaction with Multimerin-2 play an important role in pathological vascularization of the choroid, disclosing new possibilities for therapeutic intervention to neovascular AMD.

Keywords: choriocapillaris, age-related macular degeneration, angiogenesis, neovascularization, retinal degeneration

Age-related macular degeneration (AMD) is the third leading cause (among the elderly, the major cause) of vision loss in industrialized countries.[1] As a result of the global aging of the human population, a significant increase in the number of AMD patients is expected over the next few years.[2] AMD is a heterogeneous disorder and is designated, according to progression and symptoms, as early, intermediate, or advanced disease.[3] Severe vision loss can be mainly attributed to the advanced neovascular form of AMD (nAMD), which occurs when choriocapillaris, the vasculature located posterior to the outer retina, grows and penetrates Bruch's membrane, resulting in vascular leakage, hemorrhage, and, over time, the development of fibrosis.[4] Thus, massive efforts have been dedicated to the development of antineovascular treatments for nAMD. Currently, nAMD is treated by routine intraocular injections of anti-VEGF drugs.[5] Nevertheless, although this therapy has revolutionized the treatment of nAMD providing significant visual benefits, it does not induce a persistent regression of the neovascularization, and frequent intravitreal injections are necessary to limit recurrence of the disorder.[5] Therefore, targeting different nAMD-associated factors represents a novel approach to developing combinatorial therapies that may provide enduring clinical benefits, avoiding the need for multiple treatments for nAMD patients.

The human CD93 is a single-pass transmembrane glycoprotein that belongs to group 14 in the C-type lectin domain (CTLD) superfamily of proteins involved in vascular biology.[6] CD93 expression is upregulated in the hyperproliferative endothelial cells (ECs) of blood vessels in different types of cancer.[7–9] In the activated endothelium, CD93 exhibits proangiogenic activities mainly regulating cell adhesion and

migration. Indeed, CD93 silencing impairs EC proliferation, adhesion, migration, and sprout formation,[10] and the cooperation between CD93 and dystroglycan, an adhesion molecule interacting with the extracellular matrix (ECM) protein laminin, promotes EC migration and tube formation.[11] Moreover, the cytoplasmic interaction between CD93 and moesin, which anchors CD93 to the actin cytoskeleton, is crucial for stabilizing cell adhesion and CD93 recycling, both necessary for proper EC migration.[12–14]

CD93 contributes to cell adhesion and migration through its interaction with Multimerin-2, an ECM endothelial-specific member of the EDEN family consistently deposited along the blood vessels of tumor vasculature.[9,15–17] In tumor angiogenesis, the CD93/Multimerin-2 interaction stabilizes the cell surface expression of CD93 and promotes β1 integrin activation and the fibrillar organization of fibronectin, leading to filopodia formation during the angiogenic process.[18] Therefore, CD93 neutralization may represent a new target for neovascularization inhibition in pathological contexts. In fact, we have formerly reported that an anti-CD93 monoclonal antibody (clone 4E1) was able to inhibit the formation of new blood vessels in both in vitro and in vivo experiments without affecting EC survival.[10]

Previously, we have shown that CD93 is overexpressed in ECs within choroidal neovascular membranes and that the aqueous humor of nAMD patients displays a high concentration of soluble CD93.[8] Here, we investigate the involvement of CD93 and Multimerin-2 in the neovascular progression of AMD. We show that the choriocapillaris of nAMD patients, in addition to expressing high levels of CD93, also exhibits strong Multimerin-2 deposition in the extracellular environment. Using both animal and ex vivo models, we demonstrate the important role of CD93 in the formation of new blood vessels in the choroid and highlight the relevance to hampering the CD93/Multimerin-2 interaction to block AMD-associated neoangiogenesis.

METHODS

Subjects

The described research adhered to the tenets of the Declaration of Helsinki and received Institutional Review Board/Ethics Committee approval. The included patients presented with active choroidal neovascularization (CNV) secondary to AMD. As they could not benefit from anti-VEGF therapy, they were offered autologous retinal pigment epithelium–choroid graft transplantation. CNV membranes were collected during submacular surgery as previously described.[8] Patients were treated after being informed of the nature of the treatment being offered and the potential risks, benefits, adverse effects, and possible treatment outcomes. All patients signed consent forms. Demographics and clinical characteristics of patients are reported (see Supplementary Table S1).

Animals

C57BL/6 wild-type mice were purchased from Envigo (Indianapolis, IN, USA). CD93 knockout ($CD93^{-/-}$) mice on the C57BL/6 background[19] were housed in a pathogen-free animal facility at the Nuovi Istituti Biologici di San Miniato, University of Siena, Italy, in accordance with the Institutional Animal Welfare Guidelines, Italian legislation, and the ARVO Statement for the Use of Animals in Ophthalmic

and Vision Research. The animal experiments conformed with the Guiding Principles for Research Involving Animals and Human Beings[20] and were approved by the Local Ethics Committee of the University of Siena and the Italian Ministry of Health.

Immunofluorescent and Immunohistochemical Staining

CNV membranes were collected from neovascular AMD patients during submacular surgery. Healthy choroid tissues were obtained from two retinoblastoma female patients during surgery and a whole eye from the corpse of a male who died in a car accident. Samples were processed as previously described.[8,21] Immunofluorescent staining was performed with antibodies against human Multimerin-2[22] and human CD34 (QBEnd/10; Ventana Medical Systems, Inc., Oro Valley, AZ, USA). Mouse laser-injured choroids were flatmounted and stained with anti-C1qR1/CD93 (R&D Systems, Minneapolis, MN, USA) and anti-Pecam-1 (H-3; Santa Cruz Biotechnology, Dallas, TX, USA) antibodies. Primary antibodies were identified with Alexa Fluor 488 or 568 secondary antibodies (Thermo Fisher Scientific, Waltham, MA, USA). Fluorescent images were captured using a Leica TCS SP2 AOBS (Wetzlar, Germany) confocal laser-scanning microscope, and overlaid images were produced. To show colocalization events by white dots, images were processed using ImageJ software (National Institutes of Health, Bethesda, MD, USA) and the ImageJ Colocalization plug-in (threshold channel green and red 90%; ratio setting value 50%). Immunohistochemical staining was performed as previously described.[8] The primary antibodies used were against human Multimerin-2, CD34, or CD93 (monoclonal antibody 4E1).[10] Samples were counterstained with hematoxylin and images obtained with a Zeiss microscope (Carl Zeiss Meditec, Jena, Germany).

Laser-Induced CNV and Choroidal Flatmount Analyses

CNV was induced by laser photocoagulation with rupture of the Bruch's membrane as previously described.[23] Briefly, mice 8 to 10 weeks old were anesthetized by intraperitoneal injection of 2,2,2-tribromoethanol (Avertin; Sigma-Aldrich, St. Louis, MO, USA), and their pupils were dilated with 1% tropicamide. Photocoagulation lesions (100-µm spot size, 100-ms duration, 200-mW power) were delivered by the PurePoint ophthalmic diode laser system (Alcon, Irvine, CA, USA), wavelength 532 nm, coupled to a slit lamp. A coverslip was placed on the cornea as a contact lens to view the retina, and each eye received four burns centered around the optic nerve at the 3, 6, 9, and 12 o'clock positions located equidistant from the optic disk and between the major retinal vessels. The morphologic end point of the laser injury was the appearance of a bubble, which confirmed disruption of the Bruch's membrane.[23,24] Lesions in which bubbles were not observed and eyes showing hemorrhage were excluded from the study.

Seven days after laser injury, the CNV lesions were characterized using immunofluorescent staining or size measured using FITC-dextran staining in choroidal flatmounts. Briefly, mice were anesthetized and euthanized either directly for characterization or 5 minutes after a 50-µL injection of FITC-conjugated dextran (2 × 10^6 average molecular weight;

Sigma-Aldrich), dissolved in water at a concentration of 50 mg/mL, into the mouse's orbital venous sinus using a 30-gauge needle attached to a 0.3-mL syringe.[25,26] Eyes were enucleated and fixed in paraformaldehyde (3% solution) for 2 hours. The anterior segment and retina were removed from the eyecup. The remaining retinal pigment epithelium (RPE)–choroid–sclera complex was either processed for confocal immunofluorescent analysis or flatmounted in Mowiol 4-88 (Calbiochem, San Diego, CA, USA) and examined by fluorescence microscopy using an Eclipse E600 microscope equipped with a DS-Fi1c digital camera (Nikon Instruments, Melville, NY, USA). The total area of CNV associated with each rupture site was measured using Nikon NIS-Elements image analysis software. A default and constant threshold in pixels was used to quantify CNV. An operator masked to the identity of the experimental groups performed the analysis.

Mouse and Human Choroid Sprouting Assays

Dissection and culture preparation of mouse tissue were performed as previously described.[27] Briefly, 5- to 6-week-old C57BL/6J and *CD93*^{−/−} mice were sacrificed and their eyes immediately enucleated. The RPE–choroid–sclera was separated from the retina, cut into pieces, and embedded with 30 µL of growth factor-reduced Matrigel (BD Biosciences, San Jose, CA, USA) in 24-well plates. For human assay, choroid–sclera was obtained from the nasal scleral edge of eyes from the corpses of males 59, 69, and 55 years old who died of natural causes (car crash for one, heart attack for the other two). Choroids were quickly dissected, within 6 hours from the death of the individuals, and stored in M199 without supplements at 4°C until their use in the choroid sprouting assay (CSA) experiments, which were usually performed within 12 hours from collection. The choroid was cut into small pieces and embedded into 40 µL of growth factor-reduced Matrigel, in which was incorporated the monoclonal antibody 4E1 or unrelated antibodies (Mouse IgG Isotype Control, cat. no. 10400C; Thermo Fisher Scientific) at the concentration of 500 nM. Mouse and human choroidal explants were kept in a cell culture incubator (37°C and 5% CO_2) in the presence of Endothelial Cell Growth Medium 2 with supplements (PromoCell, Heidelberg, Germany). The culture medium was changed every 3 days, and on days 7 to 8 phase-contrast photographs of individual explants were captured. For immunofluorescence analysis, mouse and human choroidal explants were fixed with paraformaldehyde (3% solution) for 30 minutes and processed as previously described,[28] the only modification being that sample washes were performed on a rocker. Quantification analyses were performed in blind and measured the area of sprouting (subtracted from the explanted area) and the maximal extension of angiogenesis (from the choroid tissue edge) using the NIS-Elements image analysis software.

Statistics

Data analyses were performed with Prism 6 software (GraphPad Software, Inc., San Diego, CA, USA), and the values represent the mean ± SD obtained from at least three measurements on randomized samples. The statistical significance of the differences was determined by Student's *t*-test and the nonparametric Mann–Whitney *U* test for compar-isons between two groups. All *P* values reported were two-tailed, and $P < 0.05$ was considered statistically significant.

RESULTS

Blood Vessels of Human CNV Membranes Display Increased CD93 and Multimerin-2 Expression

It has been shown that the vascular expression of CD93, as well as its binding partner, Multimerin-2, are upregulated in several human tumor samples.[8,9,17,29–32] Similar to tumor blood vessels, choroidal neovessels from AMD patients show strong upregulation of CD93.[8] We thus wondered if Multimerin-2, the only known extracellular binding partner for CD93, was also highly deposited along the choriocapillaris of AMD patients. To address this issue, sections of CNV membranes from AMD patients already known to exhibit upregulation of vascular CD93[8] were processed for immunofluorescence analyses. Interestingly, compared to normal choroidal tissue, the choriocapillaris of AMD patients displayed a stronger expression of Multimerin-2, which overlapped that of CD34, used as a vascular marker (Figs. 1A, 1B). The differential expression of Multimerin-2 between normal and neovascular choroidal vessels and the strong CD93 expression in the choroidal neovasculature of AMD patients were confirmed by immunohistochemical analyses (Figs. 1C, 1D), indicating that Multimerin-2 is strongly deposited along blood vessels of the CNV membranes, which are characterized by the presence of proliferating ECs expressing high levels of CD93.

In Mice, the Ablation of CD93 Hinders Choroidal Angiogenesis

Because CD93 displays proangiogenic activities and its depletion impairs migration, adhesion, tube formation, and cytoskeletal organization of proliferating ECs,[7,10] we asked whether it also played a key role during the pathological vascularization of the choroid. To address this question, we exploited the *CD93*^{−/−} murine model in two different assays of choroidal neovascularization. First, we used the laser-induced CNV (LI-CNV) mouse model, which led to the formation of vascular complexes that recapitulate the main features of the exudative form of human AMD.[23] After laser photocoagulation, quantitative analysis of FITC–dextran-stained choroidal flatmounts revealed a significantly reduced neovascularization in *CD93*^{−/−} mice compared to wild-type animals (Figs. 2A, 2B). Of note, fluorescence microscopy analyses showed that, in the laser-injured regions, blood vessels from wild-type mice displayed strong CD93 staining (Fig. 2C). Strikingly, in *CD93*^{−/−} mice, no CD93 signal was observed in the laser-damaged areas, despite these regions being highly vascularized, as indicated by Pecam-1 staining (Fig. 2D). Next, to test whether the effect of CD93 knockdown on choroidal angiogenesis was a phenomenon limited to LI-CNV or could be reproduced in a different model, we employed the ex vivo choroid sprouting assay, which has been shown to be a reproducible model of choroidal angiogenesis[27] (Fig. 3A). Interestingly, the ability of the choroidal tissues to form sprouts was significantly reduced in explants from *CD93*^{−/−} mice compared to tissues explanted from control mice (Fig. 3B), as measured by a significant reduction in the area of choroid sprouting (Fig. 3C) and also in the longest vessel growth (Fig. 3D).
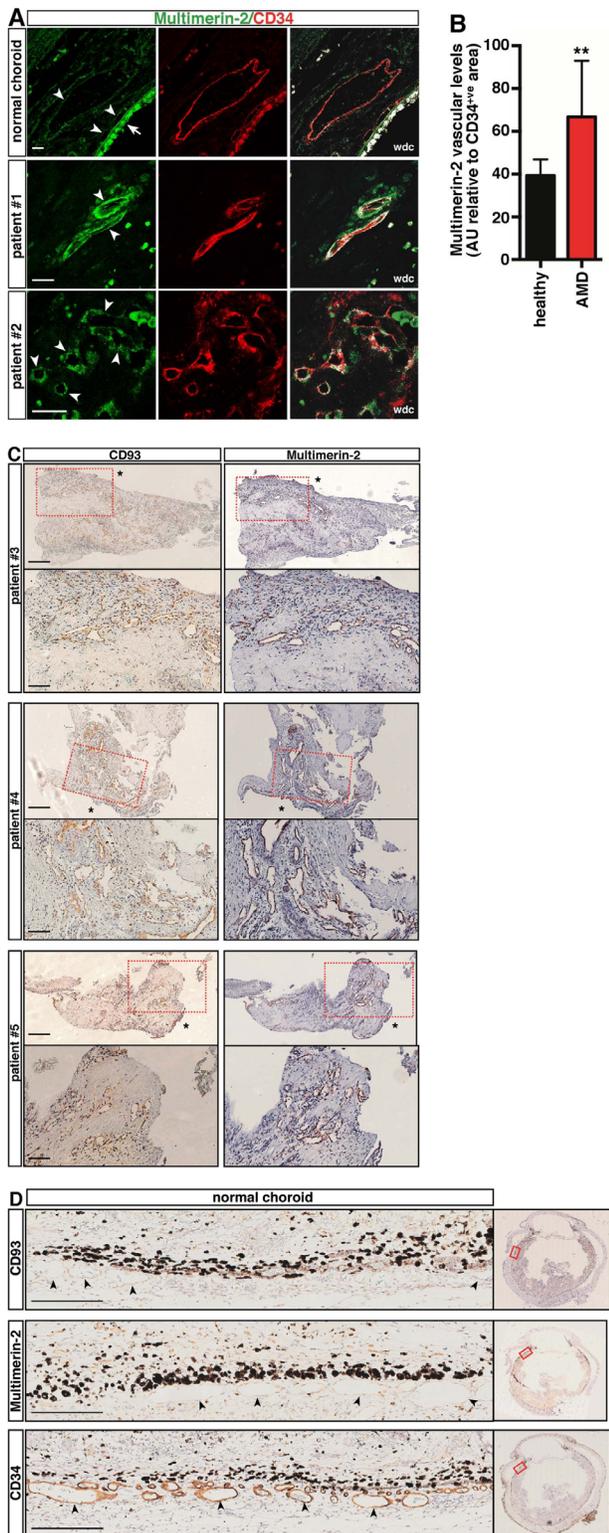
FIGURE 1. In contrast to normal choroidal tissue, CD93 and Multimerin-2 are highly expressed in blood vessels within CNV membranes. (**A**) CNV membrane sections obtained from AMD patients were analyzed by confocal imaging using antibodies to Multimerin-2 and the endothelial marker CD34. White dot colocalization (wdc) images are shown. *Arrowheads* indicate blood vessels. An *arrow* indicates the autofluorescent retinal pigment epithelium. *Scale bars*: 20 µm. (**B**) Multimerin-2 quantification in choriocapillaris from healthy ($n = 7$) and AMD ($n = 9$) patients. Values, measured using ImageJ software, represent mean ± SD expressed as arbi-

Blockage of the CD93/Multimerin-2 Interaction Prevents Endothelial Sprouting in Human Choroids

Because the binding of CD93 to Multimerin-2 has recently been demonstrated to play a pivotal role in the activation of the quiescent endothelium,[9,18] we wondered if this interaction could also promote the formation of new blood vessels in the human choroid. To address this possibility, we sought

trary units (AUs) of Multimerin-2[+ve] area normalized by CD34[+ve] area. [**]$P < 0.01$; unpaired *t*-test. (**C**) Serial CNV membrane sections were analyzed by immunohistochemistry using anti-CD93 and anti-Multimerin-2 antibodies. High magnifications of stained sections displayed in the *red dashed rectangles* are shown beneath each section. An *asterisk* indicates the most likely position of the retinal pigment epithelium, based on the presence of its small fragments. *Scale bars*: 250 µm; 100 µm for magnifications. (**D**) Serial paraffin-embedded sections from human normal choroids were analyzed by immunohistochemical staining using anti-CD93, anti-Multimerin-2, and anti-CD34 antibodies. In the left panels, *arrowheads* indicate choroidal blood vessels beneath the retinal pigment epithelium. Right panels show entire eye sections, and a *red rectangle* indicates the magnification area shown in the left panels. *Scale bars*: 250 µm.
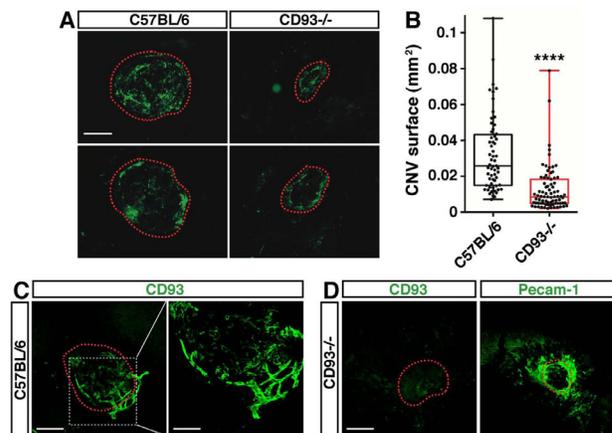

FIGURE 2. CD93 deficiency in mice associates with reduced LI-CNV. (**A**) Two representative fluorescent images of LI-CNV lesions from control (C57BL/6J) and *CD93*^{−/−} mice, captured 7 days after laser exposure. In flatmounted choroids, *red dashed lines* show the extent of the LI-CNV lesions fluorescently labeled with FITC–dextran. *Scale bar*: 150 µm. (**B**) Quantification of FITC–dextran[+ve] area in choroidal flatmounts of control (C57BL/6J, $n = 60$ impacts from 16 mice) and *CD93*^{−/−} ($n = 79$ impacts from 21 mice) mice on day 7 after laser photocoagulation. Data are presented as box-and-whiskers plots and scatterplots displaying median, lower, and upper quartiles (boxes) and minimum–maximum (whiskers) for each lesion. [****]$P < 0.0001$; unpaired *t*-test. (**C**) Choroid flatmount preparations from 7-day laser-injured regions of C57BL/6 mice were analyzed by immunofluorescence using an anti-CD93 antibody. A representative image of laser-injured areas (11 in total) from three eyes of different mice is shown. A *red dotted line* marks the LI-CNV lesion. High magnification of the stained region displayed into the *white dashed square* is shown in the right panel. *Scale bars*: 150 µm; 75 µm for the magnification. (**D**) Seven days after laser exposure, flatmounted choroids from *CD93*^{−/−} mice were fluorescently labeled with anti-CD93 and anti-Pecam-1 antibodies and analyzed by confocal microscopy. Representative images of CD93-stained (seven from two eyes of two different mice) and Pecam-1-stained (eight from the remaining two eyes of the same mice) laser-injured areas are shown. The fluorescent staining in the CD93 panel represents background noise due to secondary antibodies. *Red dotted lines* indicate the laser-injured areas. *Scale bar*: 150 µm.
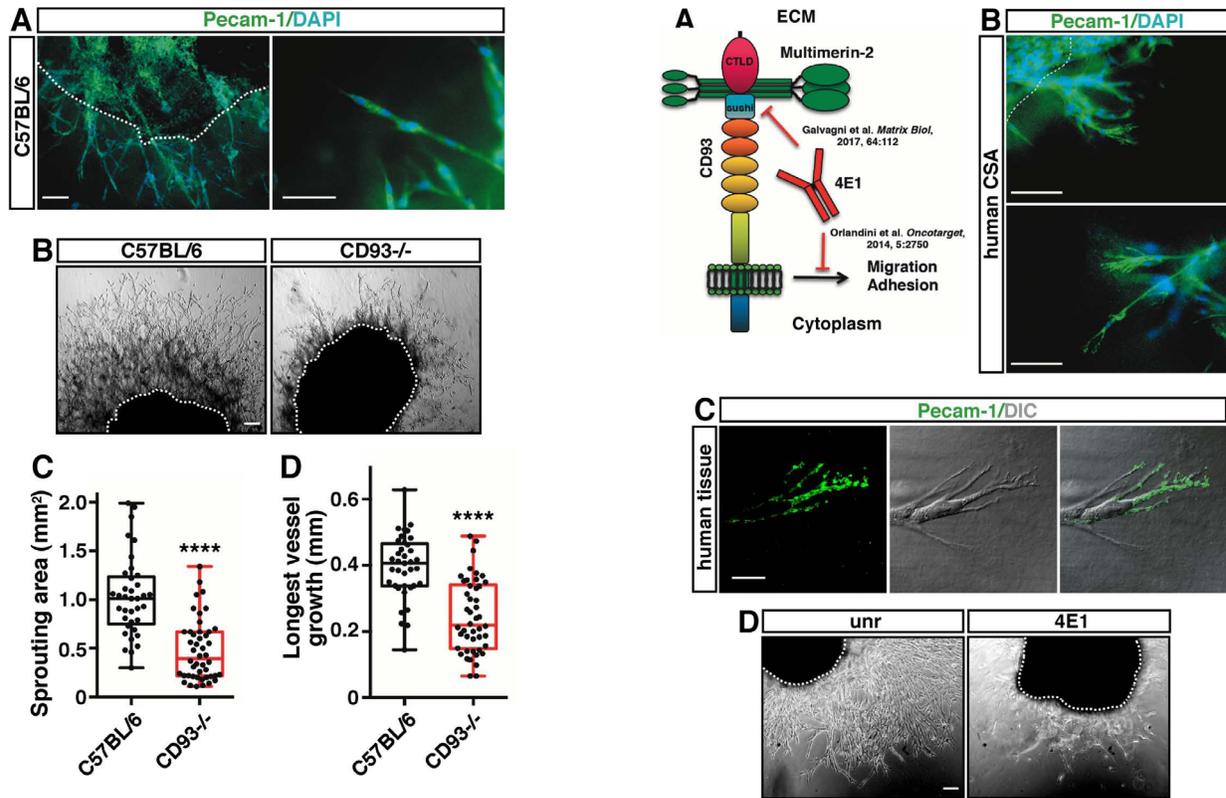
FIGURE 3. Choroidal tissue explanted from CD93$^{-/-}$ mice displays reduced EC sprouting. (**A**) Immunofluorescence analysis of choroidal sprouts from C57BL/6 mouse tissue, stained with an anti-Pecam-1 antibody and 4′,6-diamidino-2-phenylindole (DAPI) for nuclei labeling. A *dotted line* highlights the implant boundary. Images were captured using a fluorescent microscope. Details of choroidal sprouts are shown in the right panel. *Scale bars*: 50 μm. (**B**) Representative images of sprouts elicited from RPE–choroid–sclera of control (C57BL/6J) and CD93$^{-/-}$ mice. A *dashed line* indicates explant edge. *Scale bar*: 50 μm. (**C, D**) Quantitative analyses of sprouting area and maximal extension of angiogenesis from the mouse choroidal tissue edge. Data are presented as box-and-whiskers plots and scatterplots ($n = 37$ explants from four control mice; $n = 46$ explants from four CD93$^{-/-}$ mice). ****$P < 0.0001$; unpaired *t*-test.
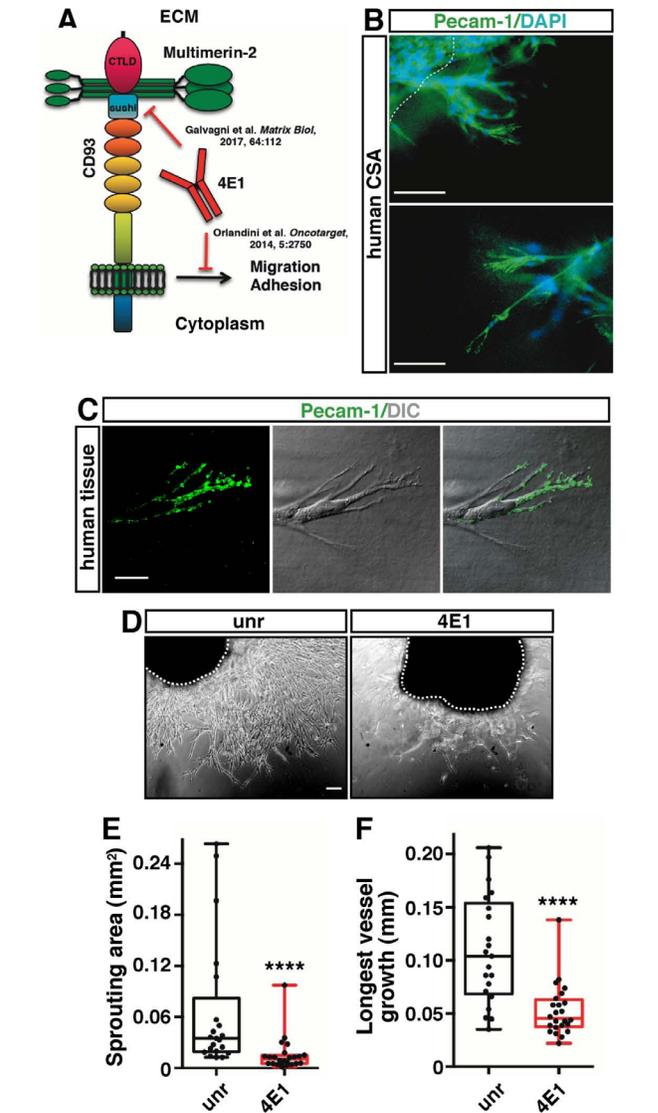

FIGURE 4. The CD93/Multimerin-2 interaction regulates human choroidal vessel sprouting. (**A**) Schematic representation of the CD93/Multimerin-2 interaction inhibition by the monoclonal antibody 4E1. The CD93 CTLD and sushi domains involved in the binding to Multimerin-2 are indicated. (**B**) Immunofluorescence staining of choroidal sprouts from human tissue, stained with an anti-Pecam-1 antibody and DAPI for nuclei labeling. A *dotted line* highlights the implant edge. Images were captured using a fluorescent microscope. Details of choroidal sprouts are shown in the lower panel. *Scale bars*: 50 μm. (**C**) Human sprouts from CSAs analyzed by confocal immunofluorescence using an anti-Pecam-1 antibody. Differential interference contrast (DIC) and overlaid images are shown. *Scale bar*: 18 μm. (**D**) Representative images of sprouts elicited from human choroids embedded into Matrigel containing the neutralizing anti-CD93 (4E1) or unrelated (unr) antibodies (500 nM). *White dashed lines* highlight the edge of choroid explants. *Scale bars*: 50 μm. (**E, F**) Quantification of sprouting area and maximal extension of endothelial sprouts from the human choroidal tissue edge. Data are presented as box-and-whiskers plots and scatterplots ($n = 21$ untreated and $n = 24$ 4E1-treated choroid explants from three cornea donors). ****$P < 0.0001$; unpaired *t*-test.

to block the binding between CD93 and Multimerin-2 in an ex vivo choroid sprouting model using the anti-CD93 monoclonal antibody 4E1, which, as we previously showed, is able to interfere with this interaction (Fig. 4A).[9] To perform the experiment, we set up a novel assay employing human tissues obtained from healthy cornea donors. Because in different mouse strains the CSA may vary significantly,[27] we compared the choroid sprouting response of human tissues with that obtained using choroids explanted from wild-type C57BL/6J mice. As observed in the mouse model, the use of the EC marker Pecam-1 highlighted the presence of vascular sprouting emerging from human explants (Fig. 4B). However, the vessel areas and vessel lengths developed from human choroids were smaller compared to those developed from the murine choroids in the same time frame (compare quantifications in Figs. 3 and 4), suggesting that both the different species and aging may be factors to slow down vascular growth we observed in human choroid. Importantly, human endothelial sprouts displayed typical tip cell features on the extending growth cones, which resemble vascular tube formation in vivo (Fig. 4C).[33] Next, to verify

the possible role of the CD93/Multimerin-2 interaction in this context, we employed the antibody 4E1 to interfere with this interaction. Importantly, and in contrast to the use of an unrelated control antibody, the presence of 4E1 significantly inhibited the ability of the choroidal tissues to form endothelial sprouts, in terms of both reduced sprouting areas and vessel length (Figs. 4D–4F).

Discussion

Following the identification of VEGF as an important regulator of nAMD, the development of anti-VEGF drugs has revolutionized the field of AMD treatment.[34] However, despite the initial therapeutic benefits, most patients develop refractory disease characterized by resumed neovascularization, eliciting the need to develop new therapeutic strategies.[35] As such, the use of combinatorial antineovascular drugs could prevent escape mechanisms and provide more effective, long-term disease control.[36]

CD93 has recently emerged as a potential target for antineovascular therapy.[16,18] Of note, CD93, along with its only currently known binding partner, Multimerin-2, were included as important components of a tumor angiogenesis signature and were found highly expressed in blood vessels within several tumor tissues of different origin.[9,37] Consistent with the aforementioned data on pathological neovascularization, we showed that CD93 and Multimerin-2 were also strongly coexpressed in blood vessels within CNV membranes of AMD patients, indicating that, during pathological vascularization of the choroid, CD93 and Multimerin-2 contribute to blood vessel growth. Importantly, CD93 and Multimerin-2 were faintly expressed in quiescent vessels of the healthy choroid. Along with our findings, a large amount of evidence suggests that the engagement of CD93 by Multimerin-2 plays a role in proliferative rather than in quiescent ECs.[9,16,18] In light of these results, low-affinity and high-avidity therapeutic agents that preferentially bind to highly target-expressing ECs could be successfully used to impair proliferative but not quiescent ECs, as has been applied to breast cancer treatment through the design of efficient, highly selective anticancer agents able to minimize toxicity.[38]

The rodent laser trauma model has contributed greatly to the present knowledge of nAMD pathogenesis, and the reproducibility of its response has encouraged studies in novel pharmacological treatments of CNV.[24] Accordingly, using the LI-CNV model in wild-type and *CD93*⁻/⁻ mice, we observed not only that the CD93 knockdown impaired the formation of new blood vessels in injured areas but also that ECs strongly expressed CD93 in wild-type laser-damaged regions, suggesting the pivotal role of CD93 during the growth of blood vessels in the process of CNV.

The relevance of Multimerin-2 in angiogenesis has been previously described, stressing its dual role as an angiostatic or a proangiogenic molecule.[16,18,22,31] These conflicting roles could be context dependent, as recently suggested by a study using the *Multimerin-2* knockout model, which highlights its role in maintaining proper blood vessel homeostasis and stabilization.[17] Therefore, through the engagement of CD93, Multimerin-2 expression may be required for vessel development in specific steps of the angiogenic process.[9,18] Accordingly, inhibiting the CD93/Multimerin-2 interaction may disrupt vascular integrity, thus retarding angiogenesis and tumor growth. In fact, the use of a Multimerin-2 recombinant peptide containing the CD93 binding site decreased

tumor growth in mouse models.[16] Also, the antiangiogenic antibody 4E1 binds between the CTLD and sushi domains, the CD93 region involved in the interaction with Multimerin-2 (Fig. 4A).[9,10] Current rodent models of CNV are still limited by the anatomical lack of a macula and by the inability to recapitulate the complex chain of events from early to late AMD.[24] In light of these observations, the possibility of inhibiting CD93/Multimerin-2 binding on human choroidal proliferative endothelium could provide important information regarding the role of this interaction in human CNV. To this end, we set up a novel experimental model based on CSA, employing human eye tissue from postmortem donors and, as a consequence, primary and not immortalized human choroidal ECs.[39] In order to maximally reduce the postmortem deterioration, human choroids were processed as quickly as possible. In all cases, despite the different ages and causes of death, in our experimental settings we observed the emergence of endothelial sprouts. Of note, blockage of the CD93/Multimerin-2 interaction by the antibody 4E1 impaired the ability of human choroidal tissues to form endothelial sprouts, reinforcing the hypothesis that hampering the CD93/Multimerin-2 interaction in the neovascularized choroid may be of potential benefit in the treatment of nAMD patients.

In conclusion, we demonstrated that choroidal human tissues obtained from healthy cornea donors might be exploited in choroid sprouting assays as effectively as the employment of rodent tissues for microvascular disease research.[27] It is currently unknown whether or not rodent models are an appropriate choice for testing humanized antibodies, and it is difficult in a preclinical setting to evaluate the toxicity and safety of potentially effective drugs for the treatment of human patients.[24,40] However, the novel experimental approach based on choroidal sprouting from postmortem eyes proposed in this study may represent a platform for appropriate testing of new pharmacological compounds for AMD treatment.

References

1. Flaxman SR, Bourne RRA, Resnikoff S, et al. Global causes of blindness and distance vision impairment 1990–2020: a systematic review and meta-analysis. *Lancet Glob Health*. 2017;5:e1221–e1234.
2. Wong WL, Su X, Li X, et al. Global prevalence of age-related macular degeneration and disease burden projection for 2020 and 2040: a systematic review and meta-analysis. *Lancet Glob Health*. 2014;2:e106–e116.
3. Coleman HR, Chan C-C, Ferris FL, Chew EY. Age-related macular degeneration. *Lancet* 2008;372:1835–1845.

4. Handa JT, Bowes Rickman C, Dick AD, et al. A systems biology approach towards understanding and treating non-neovascular age-related macular degeneration. *Nat Commun*. 2019;10:3347.

5. Mammadzada P, Corredoira PM, André H. The role of hypoxia-inducible factors in neovascular age-related macular degeneration: a gene therapy perspective. *Cell Mol Life Sci*. 2020;77:819–833.

6. Khan KA, McMurray JL, Mohammed F, Bicknell R. C-type lectin domain group 14 proteins in vascular biology, cancer and inflammation. *FEBS J*. 2019;286:3299–3332.

7. Langenkamp E, Zhang L, Lugano R, et al. Elevated expression of the C-type lectin CD93 in the glioblastoma vasculature regulates cytoskeletal rearrangements that enhance vessel function and reduce host survival. *Cancer Res*. 2015;75:4504–4516.

8. Tosi GM, Caldi E, Parolini B, et al. CD93 as a potential target in neovascular age-related macular degeneration. *J Cell Physiol*. 2017;232:1767–1773.

9. Galvagni F, Nardi F, Spiga O, et al. Dissecting the CD93-Multimerin 2 interaction involved in cell adhesion and migration of the activated endothelium. *Matrix Biol*. 2017;64:112–127.

10. Orlandini M, Galvagni F, Bardelli M, et al. The characterization of a novel monoclonal antibody against CD93 unveils a new antiangiogenic target. *Oncotarget* 2014;5:2750–2760.

11. Galvagni F, Nardi F, Maida M, et al. CD93 and dystroglycan cooperation in human endothelial cell adhesion and migration. *Oncotarget*. 2016;7:10090–10103.

12. Zhang M, Bohlson SS, Dy M, Tenner AJ. Modulated interaction of the ERM protein, moesin, with CD93. *Immunology*. 2005;115:63–73.

13. Galvagni F, Baldari CT, Oliviero S, Orlandini M. An apical actin-rich domain drives the establishment of cell polarity during cell adhesion. *Histochem Cell Biol*. 2012;138:419–433.

14. Barbera S, Nardi F, Elia I, et al. The small GTPase Rab5c is a key regulator of trafficking of the CD93/Multimerin-2/β1 integrin complex in endothelial cell adhesion and migration. *Cell Comm Signal*. 2019;17:55.

15. Zanivan S, Maione F, Hein MY, et al. SILAC-based proteomics of human primary endothelial cell morphogenesis unveils tumor angiogenic markers. *Mol Cell Proteomics*. 2013;12:3599–3611.

16. Khan KA, Naylor AJ, Khan A, et al. Multimerin-2 is a ligand for group 14 family C-type lectins CLEC14A, CD93 and CD248 spanning the endothelial pericyte interface. *Oncogene*. 2017;36:6097–6108.

17. Pellicani R, Poletto E, Andreuzzi E, et al. Multimerin-2 maintains vascular stability and permeability. *Matrix Biol*. 2020;87:11–25.

18. Lugano R, Vemuri K, Yu D, et al. CD93 promotes β1 integrin activation and fibronectin fibrillogenesis during tumor angiogenesis. *J Clin Invest*. 2018;128:3280–3297.

19. Norsworthy PJ, Fossati-Jimack L, Cortes-Hernandez J, et al. Murine CD93 (C1qRp) contributes to the removal of apoptotic cells in vivo but is not required for C1q-mediated enhancement of phagocytosis. *J Immunol*. 2004;172:3406–3414.

20. American Physiological Society, World Medical Association General Assembly. Guiding principles for research involving animals and human beings. *Am J Physiol Cell Physiol*. 2002;282:R281–R283.

21. Tosi GM, Neri G, Caldi E, et al. TGF-β concentrations and activity are down-regulated in the aqueous humor of patients with neovascular age-related macular degeneration. *Sci Rep*. 2018;8:8053.

22. Lorenzon E, Colladel R, Andreuzzi E, et al. MULTIMERIN2 impairs tumor angiogenesis and growth by interfering with VEGF-A/VEGFR2 pathway. *Oncogene*. 2012;31:3136–3147.

23. Lambert V, Lecomte J, Hansen S, et al. Laser-induced choroidal neovascularization model to study age-related macular degeneration in mice. *Nat Protoc*. 2013;8:2197–2211.

24. Pennesi ME, Neuringer M, Courtney RJ. Animal models of age related macular degeneration. *Mol Aspects Med*. 2012;33:487–509.

25. Li S, Li T, Luo Y, et al. Retro-orbital injection of FITC-dextran is an effective and economical method for observing mouse retinal vessels. *Mol Vis*. 2011;17:3566–3573.

26. Yardeni T, Eckhaus M, Morris HD, Huizing M, Hoogstraten-Miller S. Retro-orbital injections in mice. *Lab Anim*. 2011;40:155–160.

27. Shao Z, Friedlander M, Hurst CG, et al. Choroid sprouting assay: an ex vivo model of microvascular angiogenesis. *PLoS One*. 2013;8:e69552.

28. Orlandini M, Nucciotti S, Galvagni F, et al. Morphogenesis of human endothelial cells is inhibited by DAB2 via Src. *FEBS Lett*. 2008;582:2542–2548.

29. Bao L, Tang M, Zhang Q, et al. Elevated expression of CD93 promotes angiogenesis and tumor growth in nasopharyngeal carcinoma. *Biochem Biophys Res Commun*. 2016;476:467–474.

30. Olsen R, Lindh M, Vorkapic E, et al. CD93 gene polymorphism is associated with disseminated colorectal cancer. *Int J Colorectal Dis*. 2015;30:883–890.

31. Colladel R, Pellicani R, Andreuzzi E, et al. MULTIMERIN2 binds VEGF-A primarily via the carbohydrate chains exerting an angiostatic function and impairing tumor growth. *Oncotarget*. 2016;7:2022–2037.

32. Andreuzzi E, Capuano A, Pellicani R, et al. Loss of Multimerin-2 and EMILIN-2 expression in gastric cancer associate with altered angiogenesis. *Int J Mol Sci*. 2018;19:E3983.

33. Eelen G, de Zeeuw P, Treps L, Harjes U, Wong BW, Carmeliet P. Endothelial cell metabolism. *Physiol Rev*. 2017;98:3–58.

34. Bressler SB. Introduction: understanding the role of angiogenesis and antiangiogenic agents in age-related macular degeneration. *Ophthalmology*. 2009;116(suppl):S1–S7.

35. Jager RD, Mieler WF, Miller JW. Age-related macular degeneration. *N Engl J Med*. 2008;358:2606–2617.

36. Solomon SD, Lindsley K, Vedula SS, Krzystolik MG, Hawkins BS. Anti-vascular endothelial growth factor for neovascular age-related macular degeneration. *Cochrane Database Syst Rev*. 2019;3:CD005139.

37. Masiero M, Simões Filipa C, Han Hee D, et al. A core human primary tumor angiogenesis signature identifies the endothelial orphan receptor ELTD1 as a key regulator of angiogenesis. *Cancer Cell*. 2013;24:229–241.

38. Slaga D, Ellerman D, Lombana TN, et al. Avidity-based binding to HER2 results in selective killing of HER2-overexpressing cells by anti-HER2/CD3. *Sci Transl Med*. 2018;10:eaat5775.

39. Loeven MA, van Gemst JJ, Schophuizen CMS, et al. A novel choroidal endothelial cell line has a decreased affinity for the age-related macular degeneration-associated complement factor H variant 402H. *Invest Ophthalmol Vis Sci*. 2018;59:722–730.

40. Lu F, Adelman RA. Are intravitreal bevacizumab and ranibizumab effective in a rat model of choroidal neovascularization? *Graefes Arch Clin Exp Ophthalmol*. 2009;247:171–177.